

Reduction of Pb²⁺ in Aqueous Solution: Early Steps and Colloid Formation, and the Atom → Metal Transition

Arnim Henglein,* Eberhard Janata, and Anton Fojtik

Hahn-Meiter-Institut Berlin GmbH, Bereich S, 1000 Berlin 39, FRG and Heyrovsky Institute of Physical Chemistry and Electrochemistry, Academy of Sciences, Prague, ČSFR (Received: March 25, 1992)

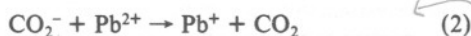
Aqueous solutions of Pb(ClO₄)₂ containing sodium formate were investigated pulse radiolytically. Pb⁺ (absorption maximum at 320 nm, $\epsilon = 2.5 \times 10^3 \text{ M}^{-1} \text{ cm}^{-1}$) is formed as the first reduction product via the reactions of e_{aq}⁻ and CO₂⁻ with Pb²⁺. The bimolecular reaction between two Pb⁺ ions to yield Pb⁰ occurs with $2k = 8.2 \times 10^9 \text{ M}^{-1} \text{ s}^{-1}$. Pb⁰ has an absorption maximum at 290 nm ($\epsilon = 1.2 \times 10^4 \text{ M}^{-1} \text{ cm}^{-1}$) and a weaker one at 660 nm ($\epsilon = 9.7 \times 10^2 \text{ M}^{-1} \text{ cm}^{-1}$). During the second-order disappearance of the Pb⁰ absorption, stronger absorption bands at shorter wavelengths build up, which are attributed to oligomeric precursors and finally metallic particles of lead. The metallic particles have an absorption maximum at 220 nm which is attributed to a plasmon oscillation. The first appearance of this band occurs at a particle agglomeration number slightly smaller than 10; thus, lead is found to possess a giant dipole oscillation band at rather small particle sizes as was first found for silver particles in solution and alkali metal particles in molecular beams.

Introduction

Monovalent lead, Pb⁺, is the first product of the radiolytic reduction of Pb²⁺ ions in aqueous solution as was shown in a pulse radiolysis study 16 years ago, and the final product is a precipitate of finely dispersed metal.¹ The present investigation was undertaken to shed light on some of the details of Pb⁺ formation, the rate of its disappearance, and the formation of further products leading to particles of metallic character. Single colloidal particles of lead have recently been shown to possess a rather narrow absorption band at 215 nm².

Small-particle research has attracted a lot of attention in various laboratories during the past few years. Such particles are investigated in the gas phase, in frozen solutions, and on various supports; studies on colloidal metal particles in solution also contribute to this field. One is interested here in surface reactions and in the accompanying optical changes³ and in the changes of the physicochemical properties in the transition range between larger metallic particles and nonmetallic clusters containing a small number of atoms.⁴ Pulse radiolysis is a method for observing the temporal development of the formation of colloidal metals. After such studies on silver, gold, and copper,⁵ we report here similar observations on colloidal lead formation.

The radiolytic reduction is brought about by the hydrated electrons, e_{aq}⁻, and reducing carboxyl radicals, CO₂⁻, which are generated in the irradiation of aqueous solutions containing sodium formate:



CO₂⁻ is formed in the attack of the OH and H radicals which are the primary products of the radiolysis of water:



The specific rate of reaction 1 is $3.9 \times 10^{10} \text{ M}^{-1} \text{ s}^{-1}$,⁶ and that of reaction 2 has been reported as $2.6 \times 10^8 \text{ M}^{-1} \text{ s}^{-1}$.⁷ The present reinvestigation of reaction 2 led to a substantially greater value of the specific rate, which means that Pb⁺ can be formed very rapidly, i.e., in a time much shorter than its lifetime with respect to the buildup of daughter products.

Experimental Section

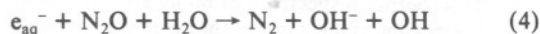
The pulse radiolysis equipment has been described previously;⁸ 3.8-MeV electrons from a Van de Graaff generator and a pulse duration of 0.5 μs were used. Extreme care was taken to prevent stray light effects in the UV measurements. UV band-pass filters (Schott) were placed between the analyzing light source and the cell, and a solar blind photomultiplier (R 166) was placed behind

the monochromator (Bausch and Lomb).

In the spectra, the absorption coefficient ϵ , which is obtained by dividing the measured absorbance change by the concentration of the species and the thickness of the optical cell (1.5 cm), is plotted versus the wavelength. For all species containing more than one lead atom, ϵ is the absorption per Pb atom. The reducing radicals, e_{aq}⁻ plus CO₂⁻, are generated with a total yield of 6 per 100 eV absorbed radiation energy.

The Pb²⁺ ion has a strong absorption band at 208 nm ($\epsilon = 8 \times 10^3 \text{ M}^{-1} \text{ cm}^{-1}$), i.e., in the region where the colloidal metal absorbs. The absorbance changes in the UV had therefore to be corrected for the consumption of Pb²⁺.

The solutions were deaerated by bubbling with argon or nitrous oxide prior to irradiation. N₂O was used if CO₂⁻ was to be the only reducing radical. In a saturated N₂O solution, the hydrated electrons are scavenged before they encounter Pb²⁺ ions,



and the OH radicals generated react according to eq 3 to yield CO₂⁻. The pH of the solutions was adjusted by adding HClO₄ or HCOOH.

Results and Discussion

Formation of Pb⁺. The specific rate of reaction 2 was determined by pulsing $(0.7\text{--}2) \times 10^{-4} \text{ M}$ Pb(ClO₄)₂ solutions which contained $2 \times 10^{-3} \text{ M}$ NaCOOH and were saturated with nitrous oxide ($2.5 \times 10^{-2} \text{ M}$). Reactions 3 and 4 occurred during the pulse under these concentration conditions. After the pulse, an absorption at 320 nm was built up within a few microseconds, which is attributed to the Pb⁺ ion formed in reaction 2. The buildup followed pseudo-first-order kinetics, the half-life being reciprocally proportional to the Pb²⁺ concentration. The rate constant calculated from this increase in 320-nm absorption was found to be $1 \times 10^{10} \text{ M}^{-1} \text{ s}^{-1}$, which is very much higher than the value of $2.6 \times 10^8 \text{ M}^{-1} \text{ s}^{-1}$ previously reported by Russian authors.⁷ At a Pb²⁺ concentration of $2 \times 10^{-4} \text{ M}$, where many of the following experiments were carried out, the formation of Pb⁺ via reactions 1 and 2 was practically finished at 1 μs after the pulse.

Figure 1 shows the absorption spectrum of Pb⁺. The spectrum was determined at 1 μs after the pulse. The same spectrum was obtained regardless of whether the solution was irradiated under argon or nitrous oxide. It contains a shallow maximum at 320 nm which has already been reported previously^{1,7} ($\epsilon = 2.5 \times 10^3 \text{ M}^{-1} \text{ cm}^{-1}$). No absorption due to Pb⁺ was observed at visible wavelengths.

Appearance of Pb⁰. After the rapid absorption increase due to Pb⁺ formation, the absorption continued to increase at practically all wavelengths, although at a much lower rate. In Figure

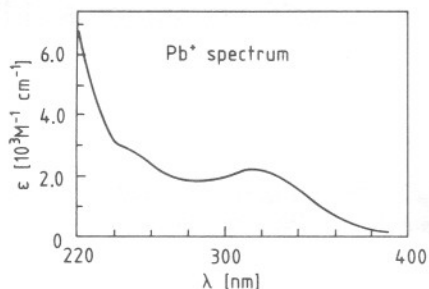


Figure 1. Absorption spectrum of Pb^+ . A solution containing 2×10^{-4} M $\text{Pb}(\text{ClO}_4)_2$, 2×10^{-3} M NaHCO_2 , and 2.5×10^{-2} M N_2O was pulsed and the absorption increase after $1 \mu\text{s}$ determined.

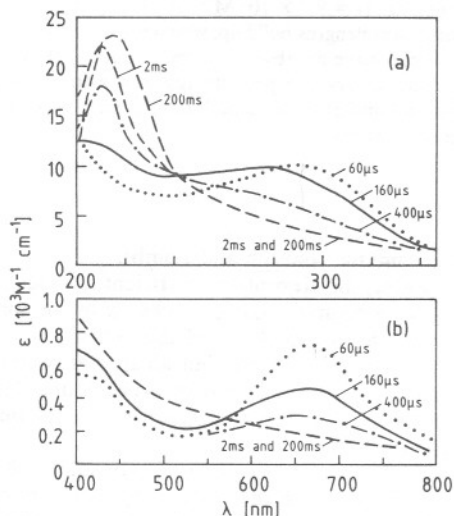


Figure 2. UV absorption spectrum (a) and spectrum in the visible (b) at various times after the pulse. Solution: 2×10^{-4} M $\text{Pb}(\text{ClO}_4)_2$; 2×10^{-3} M NaHCO_2 ; pH = 5.4. Radical (e_{aq}^- plus CO_2^-) concentration produced by the pulse: 1.1×10^{-5} M. The solution was deaerated by bubbling with argon.

2a, the absorption spectrum at $60 \mu\text{s}$ after the pulse is shown in the UV region. One can see that a product was formed which absorbs at 290 nm. However, an increase in absorption was also observed in the visible wavelength range as can be seen from Figure 2b: a maximum at 660 nm is present at $60 \mu\text{s}$, although the absorption coefficient is much lower than that of the 290-nm maximum in Figure 2a. Figure 3 shows kinetic curves at 300 and 660 nm. One can see the fast 300-nm increase due to the formation of Pb^+ (see arrow), which then is followed by a slower one. This second increase occurred more rapidly with increasing dose in the pulse. The kinetic curves could be closely fitted with second-order fits (shown by the dotted curves). As can also be seen from Figure 3, the first half-life of the 660-nm increase is a little shorter than that at 300 nm.

We attribute the buildup of the 300- and 660-nm absorptions at $60 \mu\text{s}$ to the formation of the product of the reaction of two Pb^+ ions



where the question remains open whether one is dealing with naked Pb_{aq}^+ atoms or with an atom complexed by Pb^{2+} , i.e., Pb_2^{3+} ; gaseous lead does not absorb in the visible.⁹ The Pb^0 atoms are not long lived as can be seen from Figure 3 where the absorption decays at times longer than about 0.05 ms. The buildup curves at shorter times will therefore be disturbed to a certain degree due to absorption by the daughter products. This may explain why the buildup at 300 nm occurs a little more slowly than that at 660 nm. It can also be recognized that the decay was relatively stronger at 660 than at 300 nm. If the product(s) formed in the decay of Pb^0 have strong absorption at 300 nm themselves, but relatively little absorption at 660 nm, the buildup at 300 nm can be expected to occur more slowly than at 660 nm. A close inspection of the spectra in Figure 2, a and b, at longer times reveals

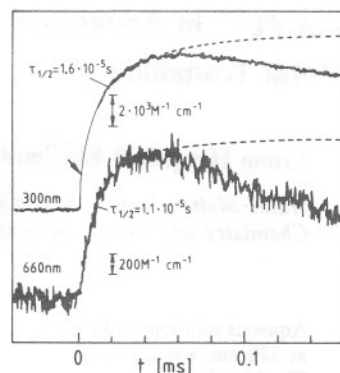


Figure 3. Kinetic curves for the buildup and beginning of decay of the absorption at 300 and 660 nm. Conditions as in Figure 2.

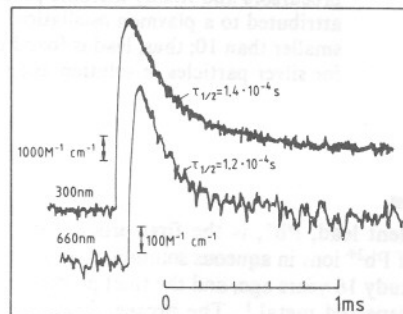


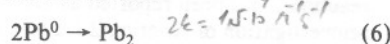
Figure 4. Kinetic curves for the decay of the 300- and 660-nm absorptions.

that the 660-nm band decays indeed more rapidly than the 300-nm absorption.

From the end value of kinetic fits such as are shown by the dotted lines in Figure 3, one obtained the following absorption coefficients of Pb^0 : $1.2 \times 10^4 \text{ M}^{-1} \text{ cm}^{-1}$ at 300 nm, and $9.7 \times 10^2 \text{ M}^{-1} \text{ cm}^{-1}$ at 660 nm. From the first half-life times in Figure 3 and concentration of Pb^+ (which is equal to the total radical concentration generated by the pulse, 1.1×10^{-5} M) one obtained the following values of the bimolecular rate constant $2k$ of reaction 5: 5.7×10^9 and $8.2 \times 10^9 \text{ M}^{-1} \text{ s}^{-1}$ when measured at 300 and 660 nm, respectively. The latter value should be more reliable because of smaller contributions from daughter products to the kinetic curve at 660 nm.

The buildup of an absorption in the 600–800-nm range has already been reported by Russian authors.¹⁰ They attributed it to the formation of Pb_2^{3+} from the reaction of Pb^+ with a Pb^{2+} ion. Our kinetic data are not in agreement with this assignment as the absorption is clearly built up via a second-order process. The rate of buildup did not depend on the Pb^{2+} concentration (in the investigated range from 1×10^{-4} to 0.5 M).

Appearance of Larger Particles. Figure 4 shows the absorptions at 300 and 660 nm as functions of time at a more compressed time scale. It can be seen that the absorptions decay within milliseconds to reach almost constant values. The rates of decay were proportional to the dose in the pulse, and the curves could be fitted closely by second-order graphs. The decay is attributed to the agglomeration of the Pb^0 atoms:



The first half-life times at 300 and 660 nm in Figure 4 are practically equal. From the first half-life of $1.2 \cdot 10^{-4}$ s in Figure 4 and the concentration of the atoms (taken as half the concentration of the reducing radicals generated in the pulse, 5.5×10^{-6} M), one calculates $2k = 1.5 \times 10^9 \text{ M}^{-1} \text{ s}^{-1}$ for reaction 6.

After 2 ms, the spectrum does not change any more at longer wavelengths (Figure 2). At this time it contains a UV absorption band quite similar to that of colloidal lead, although the band (at 210 nm) is at a slightly shorter wavelength than that of the authentic colloidal metal (at 215 nm).² At 200 ms, the band has

shifted to 220 nm, i.e., to a slightly longer wavelength; it is also not quite as high and is a little broader than the authentic one. It is concluded that 2 ms after the pulse, metal-like particles are present. The small differences between the final spectrum (at 200 ms) and the authentic spectrum of colloidal Pb are possibly due to the fact that no stabilizer was used in the present investigation; the colloidal lead particles therefore cluster together at longer times, which leads to a broadening and long-wavelength shift of the absorption band.

The spectrum at 400 μ s in Figure 2 shows that the UV band of metallic lead has already been built to an appreciable degree, but small absorption bands at 290 and 660 nm of Pb⁰ are still seen. As an approximation, the specific rate of further agglomeration processes, which lead to Pb₄, Pb₈, etc., can be assumed to be the same as that of reaction 6.¹¹ The formation of Pb₄ would then require about $2 \times 120 = 240 \mu$ s, and that of Pb₈ about $2 \times 240 = 480 \mu$ s at the dose used. This admittedly rough estimate shows that, at 400 μ s after the pulse, large particles with agglomeration numbers greater than 10 are not yet present to a noteworthy extent. It is concluded that particles with agglomeration numbers smaller than 10 already possess the strong UV band of lead, although this band is not yet fully developed and peaks at a slightly shorter wavelength than that of larger metallic particles.

In the case of the agglomeration of silver atoms, it has also been observed that the plasmon absorption band starts to develop at a particle agglomeration number close to 10.^{5a} The particles one is dealing with belong to the interesting transition range between nonmetallic clusters and metallic particles. Our observations on the early formation of giant absorption bands of metal clusters in solutions are not surprising in view of the recent observations made on metal clusters in molecular beams, where strong dipole oscillation bands reflecting the collective excitation of the Fermi

electron gas in alkali metal clusters with agglomeration numbers smaller than 10 have been detected.¹²

References and Notes

- (1) Breitenkamp, M.; Henglein, A.; Lilie, J. *Ber. Bunsenges. Phys. Chem.* **1976**, *80*, 973.
- (2) Henglein, A.; Mulvaney, P.; Holzwarth, A.; Sosebee, T. E.; Fojtik, A. *Ber. Bunsenges. Phys. Chem.*, in press.
- (3) (a) Henglein, A.; Mulvaney, P.; Linnert, T. *J. Chem. Soc., Faraday Discuss.* **1991**, *92*, 31. (b) Mulvaney, P.; Linnert, T.; Henglein, A. *J. Phys. Chem.* **1991**, *95*, 7843. (c) Henglein, A.; Mulvaney, P.; Linnert, T.; Holzwarth, A. *J. Phys. Chem.* **1992**, *96*, 2411.
- (4) (a) Henglein, A. *Chem. Phys. Lett.* **1989**, *154*, 473. (b) Mostafavi, M.; Keghouche, N.; Delcourt, M.-O.; Belloni, J. *Chem. Phys. Lett.* **1990**, *167*, 193. (c) Linnert, T.; Mulvaney, P.; Henglein, A.; Weller, H. *J. Am. Chem. Soc.* **1990**, *112*, 4657. (d) Henglein, A.; Linnert, T.; Mulvaney, P. *Ber. Bunsenges. Phys. Chem.* **1990**, *94*, 1449. (e) Henglein, A. *Isr. J. Chem.*, in press.
- (5) (a) Henglein, A.; Tausch-Treml, R. *J. Colloid Interface Sci.* **1981**, *80*, 84. (b) Mosseri, S.; Henglein, A.; Janata, E. *J. Phys. Chem.* **1989**, *93*, 6791. (c) Ershov, B. G.; Janata, E.; Michaelis, M.; Henglein, A. *J. Phys. Chem.* **1991**, *95*, 8996. (d) Ershov, B. G.; Janata, E.; Henglein, A. *Radiat. Phys. Chem.* **1992**, *39*, 123.
- (6) Baxendale, J. H.; Fielden, E. M.; Keene, J. P. *Proc. R. Soc. London, A* **1965**, *286*, 320.
- (7) Sukhov, N. L.; Ershov, B. G. *Khim. Vys. Energii* **1982**, *16*, 511.
- (8) Kumar, A.; Janata, E.; Henglein, A. *J. Phys. Chem.* **1988**, *92*, 2587.
- (9) Landolt-Börnstein *Zahlenwerte und Funktionen*; 6 Auflage, I Band, 1 Teil; Springer-Verlag: Berlin, 1950; p 122.
- (10) Ershov, B. G.; Sukhov, N. L. *Radiat. Phys. Chem.* **1990**, *36*, 93.
- (11) The increase in cross section by the increased agglomeration number is more or less counterbalanced by a lower diffusion rate; thus the assumption of a size-independent rate constant is a plausible approximation for diffusion-controlled processes in particle agglomeration.
- (12) (a) Bréchnignac, C.; Cahuzac, Ph.; Carlier, F.; Leygnier, J. *Chem. Phys. Lett.* **1989**, *164*, 433. (b) Fallgren, H.; Martin, T. P. *Chem. Phys. Lett.* **1990**, *168*, 233. (c) Wang, C. R. C.; Pollack, S.; Kappes, M. M. *Chem. Phys. Lett.* **1990**, *166*, 26. (d) Selby, K.; Kresin, V.; Masui, J.; Vollmer, M.; Scheidemann, A.; Knight, W. D. *Z. Phys. D* **1991**, *19*, 43.